DYNAMIC ANALYSISOF THE EVOLUTION LAW OF LOW-VELOCITY IMPACT DAMAGE IN COMPOSITE LAMINATES WITH A CONTINUUM DAMAGE MODEL

Peng Qu[1]*, Yuxi Jia[2]

[1] School of Mechanical & Automotive Engineering, Liaocheng University, Liaocheng 252000, China, qupeng@lcu.edu.cn
[2] Key Laboratory for Liquid-Solid Structural Evolution and Processing of Materials (Ministry of Education), Shandong University, Jinan 250061, China, jia_yuxi@sdu.edu.cn

Keywords: Impact Damage; Composite Laminates; Cohesive Zone Model; Continuum Damage Mechanics

ABSTRACT

In this paper, a numerical method for the evaluation of composite laminates damage under the low-velocity impact was proposed based on the continuum damage mechanics (CDM) and the cohesive zone model (CZM). The intra-ply damage including matrix crack and fiber fracture was represented by the constitutive model which taked into account the physical progressive failure behavior using the damage variable. The delamination at the interface between plies was characterized by the CZM which taked into account the normal crack and the tangent slip using a relation between stress and displacement The FEM which combineed the CDM and CZM bringed stable simulations, overcoming the numerical instability for the simulation of the composite laminates damage under impact. It can effectively establish the relation between the mesoscale structure and the macroscopical response under impact. The effect of interlaminar toughness on the impact damage was investigated, which have not been thoroughly discussed in most literature as yet. The numerical prediction has a good agreement with the experimental test.

1 INTRODUCTION

Fiber-reinforced polymer composite laminates have been extensively used in lightweight engineering applications, especially in modern air transportation area, due to the high specific strength and specific stiffness[1,2]. Despite of these benefits, composite laminates are susceptible to transversal impact loading because they are laminar systems with weak interface[3]. For example, in aircraft structures, low-velocity impacts are often caused by runway stones during landing or taking off and tool drops during manufacturing. The out of plane loading can cause intra-ply damage and interlaminar delamination, which result in severe drop in load carrying capacity of composite laminates. Therefore, considerable research has been done to better understand the impact properties of composite laminates[4,5].

Numerous experimental research efforts have been carried out to understand the behavior of composites under low-velocity impact applications. ASTM D 7136 is widely used to cover the damage resistance of multidirectional polymer matrix composite laminated plates subjected to a drop-weight impact event[6]. Relative to the ripe experimental method, there is a significant challenge to the numerical method for the evaluation of composite laminates damage under the low-velocity impact[7] since the hierarchical, heterogeneous structure of composite laminates give rise to a number of damage mechanisms. The fiber reinforced polymer composite laminates have three structure scales: fiber (micro-) scale, ply (meso-) scale and laminate (macro-) scale, and also have three components phase: reinforcement, matrix and interface. When the composite laminate is impacted with the foreign object, the impact dynamics in the vicinity of the impact region becomes very complex[8], with matrix crack and fiber fracture occurring in ply and delamination appearing at the interface between plies.

In this paper, a numerical method for the evaluation of composite laminates damage under the low-velocity impact was proposed based on the continuum damage mechanics (CDM) and the cohesive zone model (CZM). CDM is widely used to capture the non-linear behavior of laminates due to

damage, compared with the other theoretical formulations which are also available such as failure criteria, plasticity theory and fracture mechanics. The intra-ply damage including matrix crack and fiber fracture was represented by the constitutive model which takes into account the physical progressive failure behavior in the ply using the damage variable to describe the intra-ply damage state. The delamination at interface between plies was characterized by the CZM which takes into account the normal crack and the tangent slip using a relation between stress and displacement to describe the initiation and development of delamination based on the energy dissipation mechanisms.

2 NUMERICAL MODELLING

2.1 Intra-ply damage constitutive model

The Continuum Damage Mechanics (CDM) approach, initially introduced by Kachanov[9] and Rabotnov[10], has grown considerably in the past twenty years[7,**Error! Bookmark not defined.**,11,12,13]. Using CDM concept, Matzenmiller et al.[14] developed a mathematical model for damage of composite materials, connecting the damage level to the degraded elastic properties of the material. This approach has been implemented in many research works[15,16], demonstrating promising results in predicting the impact response and damage extent[17,18], and is used in this paper for the intra-ply damage constitutive. The lamina is treated as a homogenized continuum with the orthotropic nature of the mechanical response. Internal variables are introduced to describe the evolution of the impact damage state and as a subsequence the degradation of the material performance. The major failure mechanisms of lamina, which are accounted for in this paper involve: fiber rupture, fiber buckling and kinking, matrix cracking under transverse tension and shearing, and matrix crushing under transverse compression and shearing.

In classical continuum damage mechanics, only the undamaged (whole) part of the cross-section A (net-area) for the uniaxial case is supposed to carry loading, i.e. transmit stresses. Consequently, the stresses σ_{ij} in the failure criteria should be interpreted as effective stresses, referred to the net area. Based on the hypothesis of strain equivalence, the relation between effective stresses σ_{ij}, and nominal stress is as follow:

$$\boldsymbol{\sigma} = \boldsymbol{M}\boldsymbol{\sigma}$$

$\boldsymbol{\sigma}$ denotes effective stress tensor, M represents the rank-four damage operator, and σ denotes nominal stress tensor. For the plane stress condition:

$$\boldsymbol{M} = \begin{bmatrix} \frac{1}{1-\omega_{11}} & 0 & 0 \\ 0 & \frac{1}{1-\omega_{22}} & 0 \\ 0 & 0 & \frac{1}{1-\omega_{12}} \end{bmatrix}$$

ω_{11} is associated with longitudinal (fiber) failure, whereas ω_{22} is the damage variable associated with transverse matrix cracking and ω_{12} is a damage variable influenced by longitudinal and transverse cracks. The two damage parameters （ ω_{11} and ω_{22} ） assume different values for tension (ω_{11}t and ω_{22}t) and compression (ω_{11}c and ω_{22}c) in order to account for the phenomenon of one-sidedness. In contrast to ω_{11} and ω_{22} the damage parameter for shear ω_{12} is independent of the sign of the shear stress τ. The compliance tensor for the damaged lamina is:

$$\boldsymbol{H(\omega)} = \begin{bmatrix} \frac{1}{(1-\omega_{11})E_{11}} & -\frac{\upsilon_{21}}{E_{11}} & 0 \\ -\frac{\upsilon_{12}}{E_{22}} & \frac{1}{(1-\omega_{22})E_{22}} & 0 \\ 0 & 0 & \frac{1}{(1-\omega_{12})G} \end{bmatrix}$$

E_{11} denotes longitudinal Young's modulus, E_{22} denotes transverse Young's modulus, G denotes shear

modulus, υ denotes Poisson's ratio. The shape of the loading surface is:

$$f_{\square} = \frac{\sigma_{11}^2}{\left(1-\omega_{11c,t}\right)^2 X_{c,t}^2} - r_{\square c,t} = 0 \text{ for fiber damage model,}$$

$$f_{\perp} = \frac{\sigma_{22}^2}{\left(1-\omega_{22c,t}\right)^2 Z_{c,t}^2} + \frac{\tau^2}{(1-\omega_{12})^2 S_c^2} - r_{\perp} = 0 \text{ for matrix damage model.}$$

r denotes damage threshold, $X_{c,t}$, $Z_{c,t}$ and S_c denote longitudinal, transverse and shear longitudinal strength, respectively, subscript 'c' denotes compression and 't' denotes tension.

Since the damage variables have no direct relation to the micromechanics crack and void growth, they are treated as phenomenological internal variables for the thermodynamics of irreversible processes. Therefore, the thermodynamic conjugate force to the damage variables is:

$$\boldsymbol{Y} = -\frac{\partial \boldsymbol{W}}{\partial \boldsymbol{\omega}}$$

$\boldsymbol{W}$ denotes the strain energy function. In continuum damage mechanics the variable $\boldsymbol{Y}$ has the meaning of energy, released per volume, due to the advancement of damage. In the space of the thermodynamic forces $\boldsymbol{Y}$, a damage potential $\boldsymbol{Q}(\boldsymbol{Y},\boldsymbol{\omega})$ is introduced and the gradient of $\boldsymbol{Q}$ defines the vector-valued function for the damage rule:

$$\dot{\boldsymbol{\omega}} = \sum_i \phi_i \frac{\partial Q_i}{\partial \boldsymbol{Y}}$$

The scalar functions $\phi_i(\boldsymbol{\sigma},\boldsymbol{\omega},\dot{\boldsymbol{\varepsilon}})$ control the amount of damage growth. The models used to simulate ply damage are thoroughly described in references[14,19] and will not be elaborated here except for their main aspects mentioned above.

2.2 Cohesive zone model (CZM) for delamination

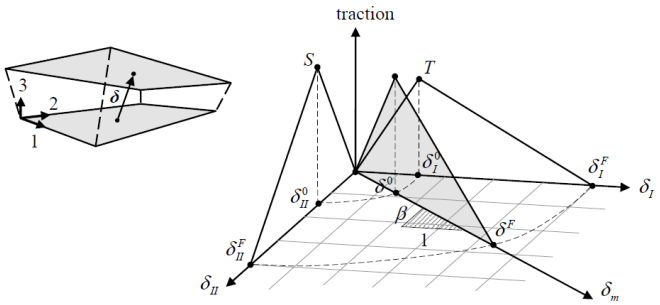

Figure 1. Cohesive zone model

The CDM does not take the delamination between plies into account. In this paper a cohesive zone damage model[20,21] is introduced to relate tractions to displacement jumps at the interface between plies[22]. Damage initiation is related to the interfacial strength, i.e., the maximum traction on the traction–displacement jump relation. When the area under the traction–displacement jump relation is equal to the fracture toughness, the traction is reduced to zero and new crack surfaces are formed, as shown in Fig. 1. For the normal delamination the fracture toughness is: $G_{IC}=0.5T\delta^F_I$ and for the tangential delamination the fracture toughness is $G_{IIC}=0.5S\delta^F_{II}$. T and S denote the peak tractions in normal and tangential direction respectively, δ^F_I and δ^F_{II} denote the ultimate displacements in normal and tangential direction respectively.

In this cohesive material model, the total mixed-mode relative displacement δ_m is defined as:

$$\delta_m = \sqrt{\delta_I^2 + \delta_{II}^2},$$

where $\delta_I=\delta_3$ is the separation in normal direction (mode I) and $\delta_{II} = \sqrt{\delta_1^2 + \delta_2^2}$ is the separation in tangential direction (mode II). The mixed-mode damage initiation displacement δ^0 is given by:

$$\delta^0 = \delta_I^0 \delta_{II}^0 \sqrt{\frac{1+\beta^2}{(\delta_{II}^0)^2 + (\beta\delta_I^0)^2}},$$

where δ^0_I and δ^0_{II} are the single mode damage initiation separations and $\beta=\delta_{II} / \delta_I$ is the mixed mode. The ultimate mixed-mode displacement δ^F for the power law is:

$$\delta^F = \frac{2(1+\beta)^2}{\delta^0}\left[\left(\frac{T}{\delta_I^0 G_{IC}}\right)^\eta + \left(\frac{S\beta^2}{\delta_{II}^0 G_{IIC}}\right)^\eta\right]^{-\frac{1}{\eta}}$$

2.3 Material parameters

The laminates used in this paper were fabricated using a fiber placement machine and Hexply AS4/8552 carbon-epoxy tows. The independent ply material properties needed for the definition of the CDM and CZM are measured by standard test methods and summarised in Table 1 which are taken from Ref. [23] directly.

Table 1 Hexply AS4/8552 ply material paremeters

E_1	E_2	G	υ_{12}	X_t	X_c	Z_t	Z_c	S	G_{IC}	G_{IIC}	ρ
GPa	GPa	GPa		MPa	MPa	MPa	MPa	MPa	N/mm	N/mm	kg/m^3
135	9.6	5.3	0.32	2207	1531	80.7	199.8	114.5	0.28	0.79	1590

2.4 Geometry and boundary conditions

Laminates test specimens of 150×100 mm^2 are fixed between a rigid support and a rigid pressure plate. Both of them have 125×75 mm^2 rectangular cuts in the center leaving part of the specimens free for impact, and are fixed during the impact process. The impactor is also modelled as a rigid body which has a spherically-shaped impact surface with a diameter of 16 mm. And it is divided into two parts, the bottom part in contact with the specimen has the practical density of steel which make the contact stiffness solution convergence available, the top part has a assumed density which make the impactor has a lumped mass equal the one used in the experiment. An initial velocity at the initiation of the contact between impactor and specimen is measured during the test and prescribed to the impactor in the simulation. Therefore, the impact energy is E=0.5mv^2, where m is the impactor mass and v is the initial velocity.

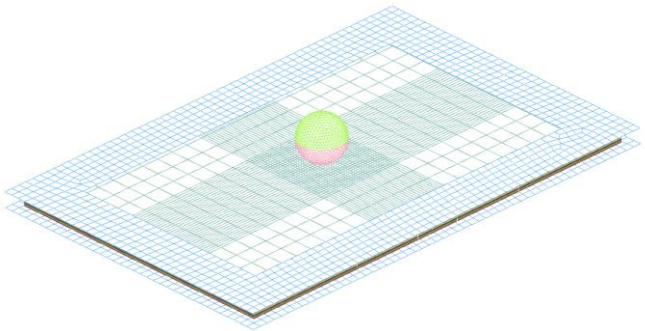

Figure 2. Finite element model

2.5 Discretization

A four-node shell element is used to discretize the lamina with the CDM constitutive model. The stacking sequence is controlled by the material angle at the integration point. The laminate is treated as a stack of shell elements. Each ply is represented by one layer of shell elements and tied together using a 'tiebreak' contact with an interface traction-displacement law which is described in CZM. After delamination, this contact behaves as a surface-to-surface contact for which no interface tension is possible to avoid interpenetration of plies. This approach gives a good approximation for delamination

stress and failure, with the advantage that the critical integration timestep is much larger since it depends on the area size of the shell elements[12]. Therefore, large composite structures can be modelled efficiently compared with the interface solid models which is more computationally expensive[12]. In regions of the model where a correct prediction of the damage initiation load is required, such as the impact zone, a fine mesh is used due to the accurate computation of the energy release (G_C) is mesh-dependent. The impactor is discretized by a eight-node solid element, and has the same mesh refinement with the impact zone of laminate.

3 RESULT AND DISCUSSION

3.1 Model verification

The 4.368mm thick specimen consists of 24 laminated AS4/8552 plies with the stacking sequence $[\pm 45/90/0/45/0_4/\text{-}45/0_2]_S$. The simulated impactor reaction force histories corresponding to 29.7J impact energy on the specimen is plotted in Fig. 3 as well as the experimental result taken from the Ref [23]. The oscillatory behavior due to the dynamic coupling between the specimen and its support, observed in the experimental tests, is not considered in this simulation, and the fitting curve of the experimental result is used to compare with the prediction result. With the increase of impact displacement, the reaction force on the impactor caused by the deforming composite specimen rapidly increases. There is an obvious drop of load at the time 0.8ms when the force is about 5500N, and it is observed both in the test and simulation. After a transient decline, the interaction force between impactor and laminates ascends again and reaches a maximum, about 5800N in test and 6000N in simulation. Then the impactor velocity is eventually reduced to zero and the impact stroke is accomplished when the ultimate displacement of impactor is 6.2mm in test and 6.8mm in simulation. The kinetic energy is completely transferred to the elastic strain energy and the dissipated energy caused by all kinds of irreversible damage in the laminates. Subsequently, the accumulated elastic strain energy is transferred back to the kinetic energy of impactor which is impelled back by the specimen. The prediction result obtained by the numerical method has a good agreement with the experimental result except that there is a little response time delay for the simulation result compared with the test result, especially for the rebound process. However, the delay of rebound does not influence the discussion of the damage evolvement which mainly occurs in the impact process.

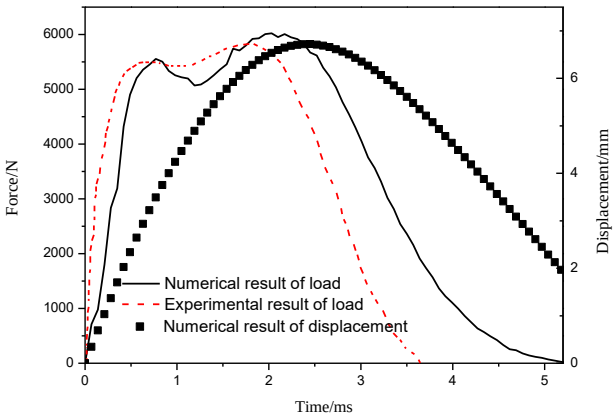

Figure 3. Impactor reaction force and displacement histories.

3.2 Delamination area

The predicted delamination area at each ply interface is shown in Fig. 4. With the increase of the impact stroke, delamination expands at all of the interface, except the one between 23th and 24th plies, which are at the top of the specimen and close to the impactor. The delamination first occurs at the interface between the 7th and 8th plies at 0.3ms, while the most of delamination initiation occurs at 0.8ms when the impact load first declines. After the time, 1.5ms, when the impact force increases again, delamination area does not increase obviously. At the end of impact stroke, 2.5ms, there is the

most delamination at the interface between 2th and 3th plies which are at the bottom of the specimen and far away from the impactor. From the top to the bottom of the specimen, the delamination area increases, which is consistent with the conic distribution of delamination under impact observed in the experiment.

The toughness of the interlaminar zone can be enhanced by the 'ex-situ' RTM toughening technology which also keeps a good manufacturability and static mechanical properties. A thin toughening layer is embedded into the interlaminar zone, and the intra-ply has the original structure. It is found that the mode I fracture toughness (G_{IC}) and mode II fracture toughness (G_{IIC}) of the composite toughened by polyamide nonwoven fabric (PNF) increase up to 1.1 times compared with those of the conventional counterparts[24]. The effect of interlaminar toughness on the impact damage is analyzed by this numerical method. As shown in the Fig. 5, as the fracture toughness is enhanced (both for the Mode I and II), the delamination area decreases under the same impact energy and with the intra-ply mechanical properties. At the end of impact stroke, the final delamination area drops 22% for the toughened 75% specimen and drops 33% for the toughened 100% specimen, compared with the no toughened specimen. The thin toughening layer can efficiently improve the delamination propagation resistance of the laminate under impact. While the initiation of delamination is not influenced by the toughening layer. It emerges at about 0.8ms for all of the three specimens.

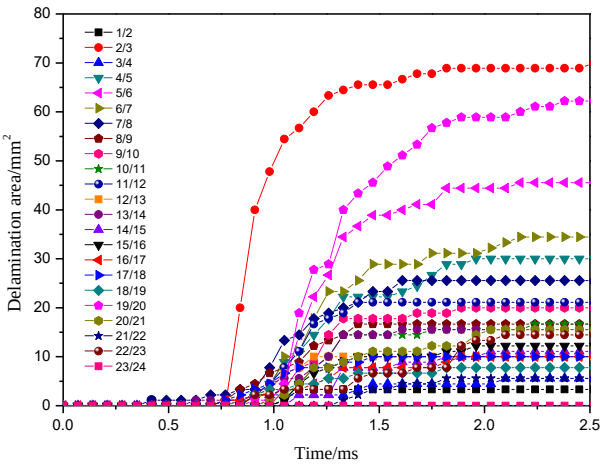

Figure 4. Delamination area for the different interlaminar zones.

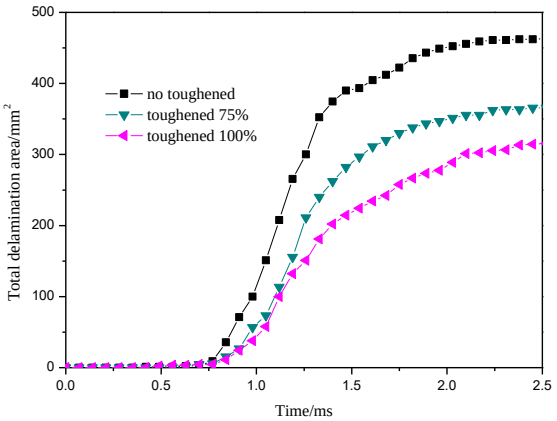

Figure 5. The effect of the interlaminar toughness on the total delamination area.

3.3 Energy dissipation

As shown in Fig. 6, the total energy of the system approximately does not vary during the impact process, which guarantees the conservation of energy in the total system. Compared with the initial energy, the kinetic energy of impactor reduces considerably when it has no interaction with laminates in the process of rebound. The specimen absorbs most of the kinetic energy with the appearance of intra-ply damage, delamination and friction between different parts. The hourglass energy maintains low level, which guarantees the accuracy of the calculation. As shown in Fig. 7, the dissipated energy caused by delamination is influenced by the interlaminar toughness. With the increase of the interlaminar toughness the dissipated energy of delamination decreases, and it is consistent with the delamination area, although the toughened specimen requires more energy per area for the propagation of delamination. There are normal delamination and tangential delamination during the impact process, and it is difficult to detect the type of delamination through experiment. Using the numerical method containing the CZM which can distinguish the type of delamination, the contribution of different delamination can be evaluated, as shown in Fig. 8. The dissipated energy of tangential delamination takes the percentage of 82% for no toughened specimen, 83% for toughened 75% specimen and 82% for toughened 100% specimen. It reveals that the shear stress is the main reason for the delamination during the impact process. The increase of interlaminar toughness can reduces the dissipated energy both for the Mode I and II, except for the Mode I of the toughened 100% specimen, of which the dissipated energy is as same as the toughened 75% specimen.

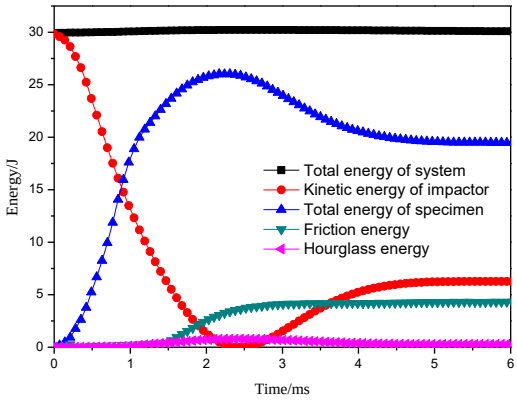

Figure 6. Energy histories.

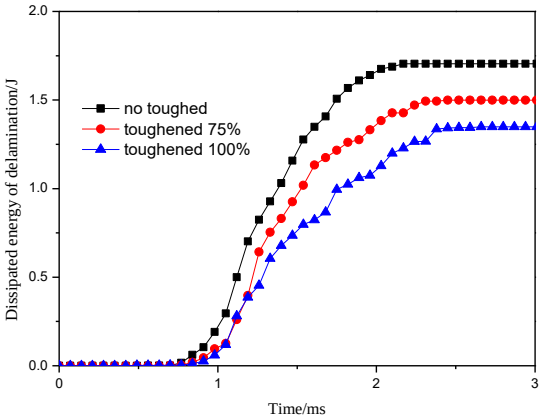

Figure 7. The effect of interlaminar toughness on the dissipated energy of delamination.

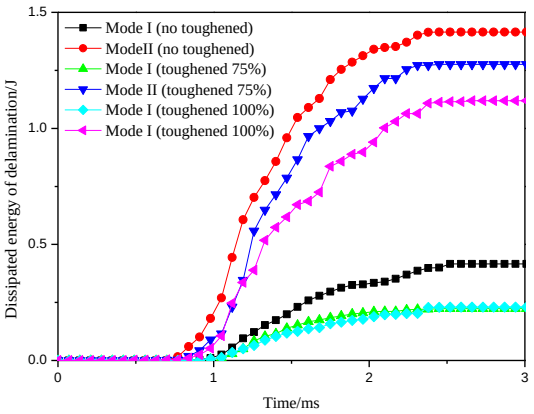

Figure 8. Dissipated energy of Mode I and Mode II delamination.

4 CONCLUSIONS

The numerical method combines the physically based continuum damage mechanics (CDM) and the cohesive zone model (CZM) , taking into account the progressive failure behavior of fibers, matrix and interfaces between plies. The prediction results obtained by the numerical method have a good agreement with the experimental results, and the FEM brings stable simulations, overcoming the numerical instability for the evaluation of composite laminates damage under the low-velocity impact.

The most of delamination initiation occurs when the impact load start to declines. To a certain extent, delamination area does not increase obviously any more. From top to bottom of the specimen, the delamination area increases. The toughness of the interlaminar affects the behavior of interfaces between plies. As the fracture toughness is enhanced, the delamination area and dissipated energy of delamination decrease. With the CZM which can distinguish the normal and tangential delamination, the contribution of different delamination can be evaluated. It reveals that the shear stress is the main reason for the delamination during the impact process.

ACKNOWLEDGEMENTS

This work was supported by the National Natural Science Foundation of China (50973056), the Natural Science Foundation of Shandong Province (JQ201016), the National Basic Research Program of China (2010CB631102), and the Independent Innovation Foundation of Shandong University (2009JQ013).

REFERENCES

[1] Peng Qu, Xiaojun Guan, Yuxi Jia, Shuai Lou and Jiaqi Nie. Effective elastic properties and stress distribution of 2D biaxial non-orthogonally braided composites. Journal of Composite Materials: 2012, 46(8), 997–1008.

[2] Peng Qu, Yuxi Jia, Jiaqi Nie and Xiaojun Guan. Comparative Analysis of Stress Distribution of Braided Composites under Different Load Conditions. Polymers & Polymer Composites: 2012, 20(1 & 2), 165-169.

[3] M.F.S.F. de Moura, A.T. Marques. Prediction of low velocity impact damage in carbon–epoxy laminates. Composites Part A: 2002, 33, 361-368.

[4] M. O. W. Richardson, M. J. Wisheart. Review of low-velocity impact properties of composite materials. Composites Part A: 1996, 9,1123-1131.

[5] David J. Elder, Rodney S. Thomson, Minh Q. Nguyen, Murray L. Scott. Review of delamination predictive methods for low speed impact of composite laminates. Composite Structures: 2004, 66, 677-683.

[6] Standard Test Method for Measuring the Damage Resistance of a Fiber-Reinforced Polymer Matrix Composite to a Drop-Weight Impact Event. Tech rep, American Society for Testing and Materials (ASTM), West Conshohocken, PA, USA, ASTM D7136/D7136M; 2005
[7] Schuecker. C., Pettermann, H. E. Fiber Reinforced Laminates: Progressive Damage Modeling Based on Failure Mechanisms. Archives of Computational Methods in Engineering: 2008, 15, 163-184.
[8] Gautam S. Chandekar, Bhushan S. Thatte, Ajit D. Kelkar. On the Behavior of Fiberglass Epoxy Composites under Low Velocity Impact Loading. Advances in Mechanical Engineering: 2010, 1-11.
[9] Kachanov LM. Rupture time under creep conditions. Izv Akad Nauk SSSR Otd Tekhn Nauk 1958;8(26-31) [in Russian].
[10] Rabotnov YN. Creep problems in structural members. Amsterdam: North-Holland; 1969. p. 822.
[11] Minh Q. Nguyen, David J. Elder, Javid Bayandor, Rodney S. Thomson, Murray L. Scott. A Review of Explicit Finite Element Software for Composite Impact Analysis. Journal of Composite Materials: 2005, 39(4), 375-386
[12] A.F. Johnson, A.K. Pickett, P. Rozycki. Computational methods for predicting impact damage in composite structures. Composites Science and Technology: 2001, 61, 2183–2192.
[13] P.F. Liu, J.Y. Zheng. Recent developments on damage modeling and finite element analysis for composite laminates: A review. Materials and Design: 2010, 31, 3825–3834.
[14] A. Matzenmiller, J. Lubliner, R.L. Taylor. A constitutive model for anisotropic damage in fiber-composites. Mechanics of Materials: 1995, 20, 125-152.
[15] Williams VK, Varizi R, Poursartip A. A physically based continuum damage mechanics model for thin laminated composite structures. International Journal of Solids and Structures: 2003, 40, 2267-300.
[16] Iannucci L. Progressive failure modeling of woven carbon composite under impact. International Journal of Impact Engineering: 2006, 32, 1013-43.
[17] Williams VK, Varizi R. Application of a damage mechanics model for predicting the impact response of composite materials. Computers & Structures: 2001, 79, 997-1011.
[18] Xinran Xiao, MarkE. Botkin, Nancy L. Johnson. Axial crush simulation of braided carbon tubes using MAT58 in LS-DYNA. Thin-Walled Structures: 2009, 47, 740–749.
[19] Schweizerhof K, Weimar K, Münz Th, Rottner Th. Crashworthiness analysis with enhanced composite material models in LS-DYNA—merit and limits. In: Proceedings of the fifth international LS-DYNA conference. Southfield, Michigan, 1998.
[20] M. Elices, G.V. Guinea, J. Gómez, J. Planas. The cohesive zone model: advantages, limitations and challenges. Engineering Fracture Mechanics: 2002, 69, 137-163.
[21] M. Fiolka, A. Matzenmiller. On the resolution of transverse stresses in solid-shells with a multi-layer formulation. Communications in numerical methods in engineering: 2007, 23, 313-326.
[22] LS-DYNA keyword user's manual. Version 971/Rev 5. Livermore, California CA, USA: Livermore Software Technology Corporation; May 2010. p. 2191.
[23] C. S. Lopes, P. P. Camanho, Z.Gürdal, P. Maimí, E. V. González. Low-velocity impact damage on dispersed stacking sequence laminates. Part II: Numerical simulations. Composites Science and Technology: 2009, 69(7-8), 937-947.
[24] Peng Zhang, Gang Liu, Xiaolan Hu, Wenming Zhao, Xiaosu Yi. Improving the compression strength after impact of RTM composites by interlaminar thermoplastic nonwoven fabric[J]. American Journal of engineering and Technology Research: 2011, 11(12), 40-43.